SINTEF A185 - Unrestricted

REPORT

Prediction of local atmospheric flows based upon the Reynolds averaged equations, applied to aviation safety

Karl J. Eidsvik

SINTEF ICT
Applied Mathematics

June 2006

SINTEF

SINTEF ICT

Address: NO-7465 Trondheim, NORWAY
Location: Alfred Getz vei 1, NTNU NO-7491 Trondheim
Telephone: +47 73 59 30 48
Fax: +47 73 59 29 71

Enterprise No.: NO 948 007 029 MVA

SINTEF REPORT

TITLE

Predictions of local atmospheric flows based upon the Reynolds averaged equations, applied to aviation safety

AUTHOR(S)

Karl J. Eidsvik

CLIENT(S)

Avinor AS

REPORT NO.	CLASSIFICATION	CLIENTS REF.	
SINTEF A185	Unrestricted	Erling Bergersen	
CLASS. THIS PAGE	ISBN	PROJECT NO.	NO. OF PAGES/APPENDICES
Unrestricted	82-14-04028-0	90A260	11
ELECTRONIC FILE CODE		PROJECT MANAGER (NAME, SIGN.)	CHECKED BY (NAME, SIGN.)
SINTEF A185.pdf		Karl J. Eidsvik K.J. Eidsvik	Karstein Sørli K. Sørli
FILE CODE	DATE	APPROVED BY (NAME, POSITION, SIGN.)	
90A260	2006-06-20	Svein Nordenson, Research Director Runar Holdahl	

ABSTRACT

The report describes the modelling of a meteorological prediction system for local flows in mountainous terrain. A suggestion of how the predictions should be interpreted for estimating the flight safety is also included.

KEYWORDS	ENGLISH	NORWEGIAN
GROUP 1	Meteorology	Meteorologi
GROUP 2	Turbulence	Turbulens
SELECTED BY AUTHOR	Flight safety	Flysikkerhet

Predictions of local atmospheric flows based upon the Reynolds averaged equations, applied to aviation safety

Karl J. Eidsvik
SINTEF IKT Anvendt matematikk

20. juni 2006

1 Background

A prediction system for the local flow in mountainous terrain have been developed (Utnes 2002, Lie et al 2003, Eidsvik et al 2004, Eidsvik 2005). The prediction is based upon synoptic scale information, which is downscaled by means of detailed information about the terrain and fully three-dimensional flow models. The flow modelling and its relevance for flying is described below.

2 Numerical Model

2.1 Reynolds Equations

The SIMRA (and UM and HIRLAM) numerical model is based on conservation of mean momentum, mass and potential temperature (Pope 2000). The expected flow may be described, in anelastic form, as in Equations 1, 2, 3. Time and spatial coordinates are t and x_i, with x_1 along the main flow and x_3 vertical. Kroneckers delta and the alternating symbol are δ_{ij} and ϵ_{ijk}. The velocity, pressure, density and potential temperature are: u_i, ρ, θ. The expected flow is $< u_i >, < \rho >, < \theta >$, and the turbulence is $(u_i', \rho', \theta') = (u_i, \rho, \theta) - (< u_i >, < \rho >, < \theta >)$.

$$\frac{\partial < \rho >< u_i >}{\partial t} + \frac{\partial}{\partial x_j} < \rho >< u_i >< u_j > + \epsilon_{ijk} f_j < \rho >< u_k >$$

$$= -\frac{\partial < p >}{\partial x_i} - < \rho > g\delta_{i3} - \frac{\partial}{\partial x_j} < \rho >< u_i' u_j' > \quad (1)$$

$$\frac{\partial < \rho >< u_i >}{\partial x_i} = 0 \quad (2)$$

$$\frac{\partial < \theta >}{\partial t} + \frac{\partial}{\partial x_j} < \theta >< u_j >= S_\theta - \frac{\partial}{\partial x_j} < \theta' u_j' > \quad (3)$$

Since the most local flow is associated with a typical Rossby number as large as: $R_o = U/f_3 L = O(20)$, the Coriolis rotation, f_i, is neglected at the SIMRA scale. Coriolis effects are only accounted for via the boundary conditions from the UM1-model. The heating, S_θ, is also neglected at the SIMRA scale.

2.2 Turbulence Closures

Until a rational turbulence model for geophysical flows is documented, we apply the most standard models from laboratory scale flows, based upon the Boussinesq approximation:

$$< u_i^{'} u_j^{'} > \approx \frac{2}{3} K \delta_{ij} - \nu_t \frac{\partial < u_i >}{\partial x_j} \tag{4}$$

Here $< K > = < u_i^{'} u_i^{'} > /2$, is the turbulent kinetic energy and $\nu_t = u_t l_t$ the turbulent viscosity coefficient. The HIRLAM- and the UM-models apply standard algebraic relations for u_t and l_t, while the SIMRA model apply dynamic relations. The characteristic turbulent velocity and lengthscale are given in terms of closure relations like: $u_t = (C_\mu^{1/2} < K >)^{1/2}$ and Equation 5. The thickness of the atmospheric boundary layer is D$\sim 0.2 u_*/f_3 \sim$1Km, so that in the bulck boundary layer the turbulent lengthscale is comparable to $l_f \sim \kappa x_3 (1 - x_3/D) \sim 100$ m.

$$l_t \approx \frac{u_t^3}{< \epsilon >} = \frac{(C_\mu^{1/2} < K >)^{3/2}}{< \epsilon >} \tag{5}$$

The SIMRA- model estimate the turbulent kinetic energy and dissipation ϵ, dynamically from Equations 6 and 7. Here $P = - < u_i^{'} u_j^{'} > \partial < u_i > /\partial x_j$, and $G = - < \rho^{'} u_3^{'} > g/ < \rho > \approx < \theta^{'} u_3^{'} > g/ < \theta >$. . The turbulent viscosity coefficient is then $\nu_t = u_t l_t = C_\nu < K >^2 / < \epsilon >$. Adjustments of the standard coefficient may commonly make predictions by standard models apparently better when applied to geophysical flows, but since such curve-fits may not be related to model accuracy , standard coefficients are applied here, $(\kappa, C_\mu, C_{\epsilon 1}, C_{\epsilon 2}, C_{\epsilon 3}, \sigma_K, \sigma_\epsilon) = (0.41, 0.09, 1.92, 1.43, 1, 1, 1.3)$, (Pope 2000).

$$\frac{\partial < K >}{\partial t} + \frac{\partial}{\partial x_j} < K >< u_j > = P + G - \epsilon - \frac{\partial}{\partial x_j} < K^{'} u_j^{'} > \tag{6}$$

$$\frac{\partial < \epsilon >}{\partial t} + \frac{\partial}{\partial x_j} < \epsilon >< u_j > = (C_{\epsilon 1} P + C_{\epsilon 3} G - C_{\epsilon 2} \epsilon) \frac{< \epsilon >}{< K >} - \frac{\partial}{\partial x_j} < \epsilon^{'} u_j^{'} > \tag{7}$$

An example of predicted turbulence intensity is shown in Figure 1. For geophysical turbulence with energetic quasi-horizontal, an-isotropic large scale eddies, it is neccesary to discuss closer what $< K >$ and $< \epsilon >$ as estimated from Equations 6, 7, should be interpreted as in this case, and we extrapapolate from what is most commonly accepted both for laboratory- and full scale geophysical flows: the structure of the smallest isotropic inertial subrange eddies. Physically $< \epsilon >$, measures the energy dissipation near Kolmogorovs microscale: $\epsilon = \nu (\partial u_i^{'} / \partial x_j)^2$, as well as the energy transfer from the large to smaller eddies and also the intensity of the Kolmogorov inertial subrange spectrum. In our context it is

physically more rational to identify the estimated $< \epsilon >$ with the characteristic length-scale of the most energetic quasi-isotropic, but also flux-containing eddies represented as in Equations 4 and 5.

The inertial subrange one-dimensional energy spectra are given in Equation 8, with the Kolmogorov coefficient $\alpha_K \approx 0.5$. As mentioned, in the present context the intensity of the small scale isotropic turbulence should rather be estimated in terms of $< K >$ and l_t than from Equation 7 directly.

$$E_{11}(k_1) \approx \frac{3}{4} E_{22}(k_1) \approx \frac{3}{4} E_{33}(k_1) \approx$$

$$\alpha_K < \epsilon >^{2/3} k_1^{-5/3} \approx \alpha_K (C_\mu^{1/2} < K > l_t^{-2/3}) k_1^{-5/3}, \quad for \quad (k_1 l_t) >> 1, \qquad (8)$$

The estimated $< K >$ is also supposed to contain energy from the quasi-isotropic and flux-containing eddies (Equation 4). Even the largest of the eddies assosiated with significant vertical velocity, contributing most to vertical fluxes $< u_i' u_3' >$, $< K' u_3' >$ and the wall stress $u_*^2 \approx C_\mu^{1/2} < K > (x_3 \rightarrow 0)$ are supposed to be included in the estimated $< K >$. It therefore follows that $< K > \approx 3/2 Q_{33}$. The spectrum of the vertical velocity component can be approximated with the Kaimal model spectrum (Equation 9 with $l_{t3} = l_t$).

$$k_1 E_{ii}(k_1) \approx \frac{Q_{ii}(0) k_1 / k_{mi}}{[1 + (3/2)(k_1/k_{mi})]^{5/3}}, \quad l_{ti} k_{mi} \approx \frac{4}{3} (\frac{3}{2})^{5/2} (\frac{\alpha_K C_\mu^{1/2} < K >}{Q_{ii}(0)})^{3/2} \quad i > 1 \qquad (9)$$

$$\frac{\sigma_1}{\sigma_3} = (\frac{Q_{11}(0)}{Q_{33}(0)})^{1/2} \sim (\frac{3}{4})^{1/2} (\frac{l_{t1}}{l_{t3}})^{1/3} \qquad (10)$$

The largest scale quasi-horizontal, an-isotropic geophysical eddies are supposed not to be contained in $< K >$ and $< \epsilon >$ as estimated from Equations 6 and 7, but it may still be convenient to include them in what we call "turbulence". These fluctuations must be estimated by means of ad hoc relations. Experimental evidence from the near bottom boundary layer over flat land suggest that the variance of u_i' is related to $< K > \approx C_\mu^{-1/2} u_*^2$, like: $Q_{11}(0) \approx Q_{22}(0) \approx 4.5 u_*^2 \approx 1.4 < K >$, $Q_{33}(0) \approx 1.7 u_*^2 \approx 0.5 < K > \sim (2/3) < K >$ (Phanofsky and Dutton 1984, Kaimal and Finnigan 1994). This means that $\sigma_1 / \sigma_3 \sim 1.7$. Very approximately the Kaimal spectrum (Equation 9 and 10) is also fruiteful for the horizontal velocoity components and temperature, so that the σ_1/σ_3-ratio of 1.7 corresponds to $l_{t1}/l_{t3} \sim 7.0$ (Equation 10). Other data suggest that the one-dimensional spectra for the horizontal velocity components and temperature tend to follow -5/3 spectral laws (Equation 8, 9) farther beyond $k_{m3} \sim 1/l_{t3}$, say to $k \sim 1/l_{t1} \approx 1/l_{t2} \approx 1/D \approx 1/1Km$ (Panofsky and Dutton 1984, Kaimal and Finnigan 1994) and on the long time average even to 1/100 Km (Lindborg and Cho 2001). Such lengthscale relations will vary significantly with the height and stratification. Since the large scale contribution is supposed to be associated with small vertical velocity, it contribute little to vertical fluxes and wall stress, so it may not be dynamically essential. This is one reason why there may be some hope that a standard turbulence model developed and tuned to laboratory-scale flows may be applicable also to weakly stratified full-scale geophysical flows.

Other aspects of the flow may be more conveniently discussed in terms of the covariance function $Q_{ij}(\triangle \mathbf{x}) =< u_i'(\mathbf{x}) u_j'(\mathbf{x} + \triangle \mathbf{x}) >$ or the structure function $D_{ij}(\triangle x)$, which can

be approximated as in Equation 11. The Kolmogorov coefficient is: $\alpha_{K*} \approx 4\alpha_K \approx 2.0$ (Pope 2000). Here the structure function for horizontal velocity components is assumed to approach a saturation level, $2Q_{ij}(0)$ for $|\triangle x_i| > l_{t1}$, but the larger scale structure function for two-dimensional turbulence is also estimated to increase like $\alpha_{K*}(<\epsilon>|\triangle \mathbf{x}|)^{2/3}$, with a large scale coefficient of about $\alpha_{K*} \sim 5.5$ (Lindborg and Cho 2001).

$$D_{ij}(\triangle x) =< [u_i(\mathbf{x}+\triangle \mathbf{x}) - u_i(\mathbf{x})][u_j(\mathbf{x}+\triangle \mathbf{x}) - u_j(\mathbf{x})] >= 2(Q_{ij}(0) - Q_{ij}(\triangle \mathbf{x}))$$

$$\sim Min[\alpha_{K*}(C_\mu^{1/2} < K >)(\frac{|\triangle \mathbf{x}|}{l_{t3}})^{2/3}[\frac{4}{3}\delta_{ij} - \frac{1}{3}\frac{\triangle x_i \triangle x_j}{(\triangle x)^2}], 2Q_{ij}(0)] \qquad (11)$$

Numerical modelling of geophysical flows normally have to be on too sparce grids, and even the smallest scale of a nested prediction system may be so. This implies that the turbulence intensity $\sqrt{K}$ is underestimated. This is so because the turbulent production is proportional to the mean wind shear squared ($P \approx u_t l_t(\partial < u_i > /\partial x_j)^2$), which focuses the smallest scale variations. Smaller grids will therefore tend to give larger turbulent production and turbulence intensity. However, in idealized lee wave flow with rotors the estimated maximum $\sqrt{K}$ turns out to be fairly constant as long as $\triangle x_1 < 0.5 L_3$ (Eidsvik 2005). When the grid is larger the turbulence cannot be estimated accurately so that simple turbulence closures can be applied.

2.3 Stochastic Variations along Trajectories

When the atmospheric fields are nearly Gaussian, their stochastic properties are specified by their mean- and covariance- fields. The stochastic velocity fluctuations along a trajectory (such as a long final), can be modelled roughly as a Gaussian autoregressive processes (Box and Jenkins 1970), with parameters supposed to vary slowly along the trajectory. The autoregressive coefficients $\phi_{ij}(p)$ are given from the covariance function $Q_{ij}(p\triangle x)$ by means of Yul Walker's equation.

$$\sum_{p=0}^{P} \phi_{ij}(p) u_j'(x - p\triangle x) = w_i(x), \qquad \phi_{ij}(0) = \delta_{ij} \qquad (12)$$

For the purpose of illustration, the velocity components are supposed to be stochastically independent with exponential instead of power-law covariance function $Q_{ij}(\triangle x) \propto \delta_{ij} exp(-p\triangle x/l_{ti})$. The autoregressive coefficients can then be assigned a simpler notation so that for each i: $\phi_{ij}(p) = \phi_i(p)\delta_{ij}$. The length-scales are estimated from Equation 5 and $l_{t1} \sim l_{t2} \sim D \sim 1$ Km. In this study the simplest first order autoregressive process (P=1) is applied, so that the coefficients are given in Equation 13. Realizations of $u_i'(x)$ can then be simulated by means of a random number generator for the white Gaussian $w_i(x)$.

$$-\phi_i(1) \approx exp(-\triangle x/l_{ti}), \qquad < w_i'(x) w_i'(x) > \approx < u_i'(x) u_i'(x) > (1 - \phi_i(1)^2) \qquad (13)$$

Examples of realizations of turbulence corresponding to the expected flow in Figure 1 are given in Figure 2.

3 Meteorological Norms for Flight Safety

3.1 Wind-shear

The dynamics and control of flight are classical scientific subjects (Stengel 1994, 2004). Simplified norms for flying safety are the F-factor, the intensity of the turbulent energy spectrum and the crosswind component near the runway (Clark et al 1994, Proctor and Hinton 2000). The F-factor is relevant for the change along the trajectory of the aeroplane potential and kinetic energy relative to the flow, in geophysical notations:

$$\frac{d(1/2(c-u_1)^2+gx_3)}{dt} \approx cg[\frac{Tr.}{gM}+[-\frac{c}{g}\frac{\partial u_1}{\partial x_1}+\frac{u_3}{c}]]$$

Here the aeroplane ground speed, mass are and trust-drag are c, M, and Tr. The F-factor is: $F=[-(c/g)\partial u_1/\partial x_1+u_3/c]$. If the F-factor is too small over a sufficiantly long distance l_f, and sufficient trust is not added soon enough or is not available, the energy loss may be so large that it cannot be stopped. As originally defined in the Equation above, the windshear term has a spectrum like the spectrum of u_1 (Equation 8) times the wavenumber to the second power. This means that the F-spectrum have a maximum near Kolmogorovs microscale, which is obviously irelevant for the energy of the aeroplane. The averaging over l_f, in Equation 14 is supposed to represent a more realistic lengthscale for energy responce. The faster and larger the aeroplane (c, l_f), the more important the windshear term. For conventional airliners in landing configuration the speed is typically: $c \approx$75 m/s and the response time and distance is comparable to $t_f \sim$7 s, $l_f \sim ct_f \sim$ 0.5 km. The available trust ratio is comparable to 0.15, but delays in recognition of a wind-shear situation suggest that the response distance should be larger, and the FAA-standard for jet transports is $l_f=$ 1Km. The corresponding alert F-factor is about -0.05 an the hazardous F-factor is -0.1 (Proctor and Hinton 2000). For the Hong Kong wind-shear warning system this corresponds to a wind-shear of 15 m/s beeing considered as hazardous and alerts are already issued when the estimated wind-shear is larger than 7.5 m/s (Shun 2003).

$$F=-\overline{\frac{c}{g}\frac{\partial u_1}{\partial x_1}+\frac{u_3}{c}}^{l_f} =-\frac{c}{gl_f}[u_1(x_1+l_f/2)-u_1(x_1-l_f/2)]+\frac{\overline{u_3}^{l_f}}{c} \qquad (14)$$

Examples of realizations of the F-factor is given in Figure 3. Although u_1 may be almost Gaussian, with a Kurtosis equal to 3, the derivetive $\partial u_1/\partial x_1$, and the difference $[u_1(x_1+l_f/2)-u_1(x_1-l_f/2)]$, may have a Kurtosis as large as $R_t^{3/16}=(u_t l_t/\nu)^{3/16} \sim$20 (Pope 2000). The probability of extreme and hazardous F-values are therefore significantly larger than for a Gaussian process. Nevertheless, for the purpose of approximative estimation, we imagine that the distribution of F (conditional to known mean flow) is quite Gaussian and spesified in terms of its mean and variance. When the flight trajectory and the 1-direction are specified, the expected value of F can be estimated from the numerical model like in Equation 15.

$$<F>=-\frac{c}{gl_f}[<u>_1\,(x_1+l_f/2)-<u>_1\,(x_1-l_f/2)]+\frac{1}{c}\overline{<u>_3}^{l_f} \qquad (15)$$

The variance of F is estimated in Equation 16. Both $< K >$, and the dissipative length-scale l_{t3}, are estimated in the numerical model (Equations 6, 7 and 5). If the flow is dominated by specific structures such as microbursts or gust fronts, the expected value (Equation 15) may be most important, but in locally homogeneous flows with intense turbulence, the stochastic variation is normally largest (Equation 16).

$$< F'^2 > \approx (\frac{c}{gl_f})^2 D_{11}(l_f) + \frac{2l_{t3}}{l_f}[1 - \frac{l_{t3}}{l_f}(1 - exp(-\frac{l_f}{l_{t3}}))]\frac{Q_{33}(0)}{c^2}$$

$$\sim [0.5(\frac{c^2}{gl_f})^2(\frac{l_f}{l_{t3}})^{2/3} + 3.4\frac{l_{t3}}{l_f}]\frac{(C_\mu^{1/2} < K >)}{c^2}$$

$$\sim [0.5(\frac{c^2}{gl_{t3}})^2(\frac{l_{t3}}{l_f})^{1/3} + 3.4]\frac{l_{t3}}{l_f}\frac{(C_\mu^{1/2} < K >)}{c^2}, \quad for \;\; 1 < \frac{l_f}{l_{t3}} < 10 \tag{16}$$

3.2 Turbulent Forcing, Flight Control

With a linear airplane response, the spectrum of forcing is proportional to the wind spectrum (Equations 8 and 9). At a given frequency relative to the aeroplane $\omega \approx k_1 c$, the forcing spectrum in the inertial subrange is then proportional to:

$$E_{11}(\omega) \approx \alpha_K < \epsilon >^{2/3} c^{2/3}\omega^{-5/3},$$

so that the linear forcing is proportional to $< \epsilon >^{1/3} c^{1/3}$. This forcing may load the aeroplane and give attitude variations, which have to be controlled by means of elevator, rudder and ailerons. Too large $< \epsilon >^{1/3}$ may therefore give structural damage or loss of attitude control. For commercial aircrafts at a cruising speed $c \approx$250 m/s, a value of $< \epsilon >^{1/3}$ smaller than about 0.3 $m^{2/3}s^{-1}$ is considered as light turbulence, values in the interval $(0.3 - 0.5)m^{2/3}s^{-1}$ as moderate turbulence and values larger than about 0.5 $m^{2/3}s^{-1}$ is considered as severe turbulence (Clark et al 1997. ICAO). In terms of the turbulent intensity and length-scale this norm can be expressed like below (Pope 2000), so that a turbulent field characterized with (in SI-units): $\sqrt{< K >} > 0.75 l_t^{1/3} \sim 3.5$ m/s, is to be considered as severe. It is to be noted from Equations 16 and 17 that both the stochastic part of the wind-shear and structural norms depend quite similarly upon the model variables $< K >$ and l_t. It should be kept in mind that the "instantaneous dissipation rate" $\epsilon = \nu(\partial u_i'/\partial x_j)^2$, is approximately log-normally distributed with a variance like the velocity-derivative Kurtosis, as large as $< (\epsilon - < \epsilon >)^2 > / < \epsilon >^2 \sim R_t^{3/16} \sim$20 (Pope 2000). For a given $< \epsilon >$, extreme and intermittent ϵ-values and forcing do therefore occur more commonly than for a Gaussian variable.

$$< \epsilon >^{1/3} \approx (\frac{(C_\mu^{1/2} < K >)^{3/2}}{l_t})^{1/3} \approx 0.67 < K >^{1/2} l_t^{-1/3} \tag{17}$$

Near the landing and departure the wind conditions may also be unacceptable because of to large crosswind component near the ground. We are not familiar with commonly accepted norms for this, so we suggest that the crab angle near tuchdown ϕ_C, as given in Equation 18 may be relevant. For conventional commercial aircrafts the stall speed is

about $c_s \approx$50 m/s an expected crosswind component of $< u_2 > \sim$ 10m/s, corresponding to $< \phi_C > \approx$ 10 deg, is normally considered to be large. In moderate turbulence conditions, with $\sqrt{K} \sim 2.5$ m/s, the crab angle will then also have a standard deviation comparable to $\sigma_\phi \approx$2.5 deg, so that if "accurate control" were possible, the crab angle would exceed the interval $2 < \phi_C < 18$deg with a probability comparable to 10^{-3}.

$$< \phi_C >= Arsin(\frac{< u_2 >}{c_s}), \qquad \sigma_\phi \approx Arsin(\frac{\sigma_2}{c_s}) \tag{18}$$

At a given occasion, flying safety requires that there is an acceptably small probability of exceeding limits of F, $\epsilon^{1/3}$ and crosswind component. If the predicted "local weather conditions", with prediction errors accounted for, give too large exeedance probability, flying may be hazardous.

3.3 Probability of False Warnings

For general confidence, a system for low level wind-shear warnings should preferably predict a correct warning with a large probability and a false warning with a small probability. Although this is commonly applied as an important design criterium, it appears that it could be difficult to achieve with any prediction method.

One reason is that both the F and $\epsilon^{1/3}$-norms have large variance and Kurtosis. This means that the probability of extreme values are large, so that hazardous conditions can occur even if the average conditions are not very "extreeme".

Warning techniques based upon estimating actual values of F by means of local observations of various kind, must have similar properties. Since the spectrum of velocity differences is almost white, the wind-shear over l_f can only be estimated with considerable uncertainty, say like expressed from a Markovian shear model. The wind-shear estimation error is then comparable to $1.4\sqrt{K}$. In addition the Kurtosis is still large so that hazardous conditions can occur even if the average conditions are not very "extreeme".

It therefore appears that a significant level of false warnings should be accepted as normal with any prediction method.

4 References

Box G.E.P, Jenkins G.M. (1970). Time Series Analysis, Forecasting and Control. Holden Day 553 pp.

Clark T.L., Keller T., Coen J., Neilley P., Hsu H.-M., Hall E.D. (1997): Terrain-Induced Turbulence over Lantau Island: 7 June 1994 Tropical Storm Russ Case Study. J. Atmos. Sci. Vol 54 pp 1795–1814

Eidsvik K.J., Holstad A., Lie I., Utnes T. (2004): A Prediction System for Local Wind Variations in Mountainous Terrain. Boundary Layer Meteorology Vol 112 pp 557–586

Eidsvik K.J.(2005): A system for Wind Power Estimation in Mountainous Terrain. Prediction of Askervein Hill Data. Wind Energy Vol 8 pp 337–249

Kaimal J.C., Finnigan J:J (1994): Atmospheric Boundary Layer Flows, Their Structure and Measurement. Oxford University Press 1994.

Lie I., Utnes T., Blikberg R. (2003). On preconditioned iterative solution of distributed sparse linear systems in SIMRA. *http://balder.ntnu.no/ttp*

Lindborg E., Cho J.Y.N. (2001) Horizontal velocity structure functions in the upper troposphere and lower stratosphere. ". Theoretical considerations. Journal of geophysical research Vol 106 no D10. pp 10233–10241

Panofsky H.A.and Dutton J.A. (1985): Atmospheric Turbulence.John Wiley,New York. 397pp.

Pope S.B. (2000): Turbulent Flows. Cambridge University Press 771 pp

Proctor F.H., Bracalente E.M., Harrah S.D., Switzer G.F., Britt C.L (1995): Simulations of the 1994 Charlotte Micro-burst with Look-Ahead Wind-shear Radar. 27-th Conference on Radar Meteorology, Vail Co, USA, 9-13 Oct. 1995, Paper-10B,7

Proctor F.H., Hinton D.A. (2000): A Wind-shear Hazard Index. Preprints of 9th Conference on Aviation, Range and Aerospace Meteorology. 11-15 Sept 2000, Orlando Florida. American Meteorology Society

Shun C.M. (2003): Ongoing research in Hong Kong has led to improved wind shear and turbulence alerts ICAO Journal Vol 58 no 2 pp 1–9

Stengel R.F. 1994. Optimal Control and Estimation. Dover Publications New York

Stengel R.F. 2004; Flight Dynamics. Princeton University Press 845 pp

Stratton D.A., Stengel R.F 1993: Robust Kalman Filter Design for Predictive Wind Shear Hazard Assessment, *IEEE Transactions of Aerospace and Electronic systems, Vol 29,4 pp 1185–1194*

Utnes T. (2002): Numerical formulation of a semi-implicit Reynolds-averaged model (SIMRA). SINTEF Applied Mathematics

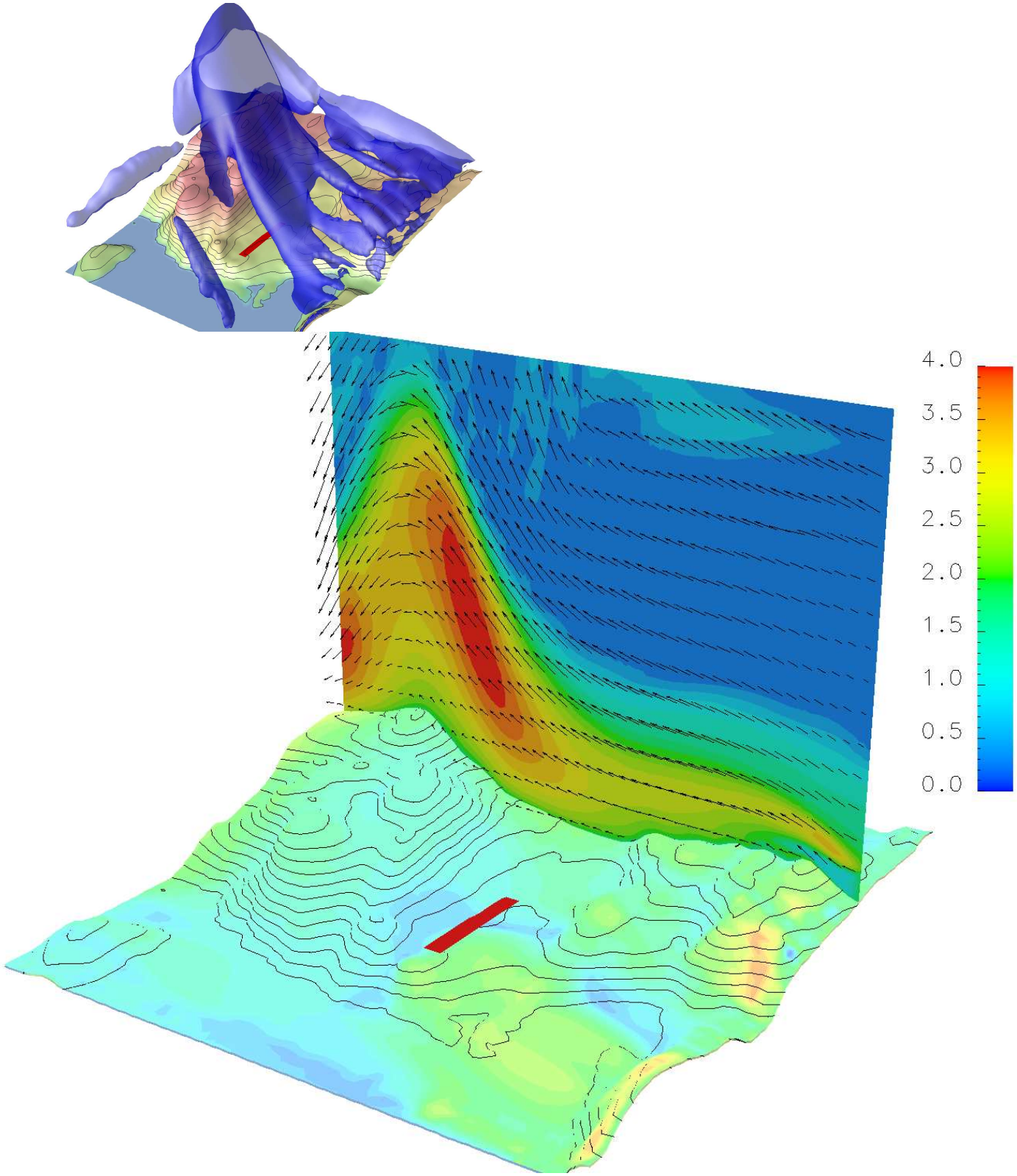

Figur 1: Predicted turbult intensity, $\sqrt{K}$. Upper: isosurface for $\sqrt{K} = 3.0$ m/s. Lower: turbulent intensity along ground and along vertical cross section Color scale for $\sqrt{K}$ (m/s). Grid resolution $\triangle x_1 \approx 35$m

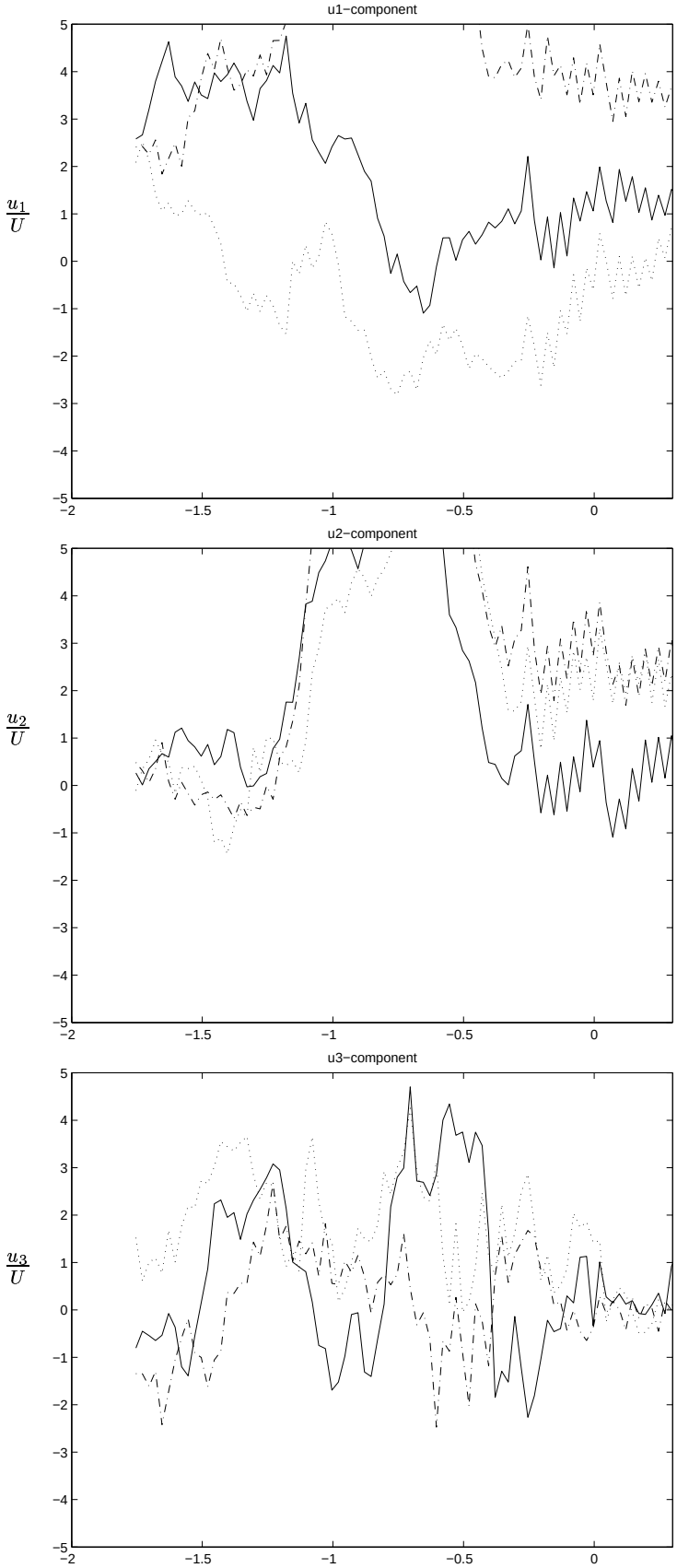

Figur 2: Three realisations of longitudinal-, transversal- and vertical wind components along the final to runway 05 Hammerfest, 1-5-05 kl 14:00. The standard deviations and lengthscales are extrapolated from $\sqrt{K}$ and ϵ as indicated in the text. Distance from treshold in km. Grid resolution as in Figure 1.

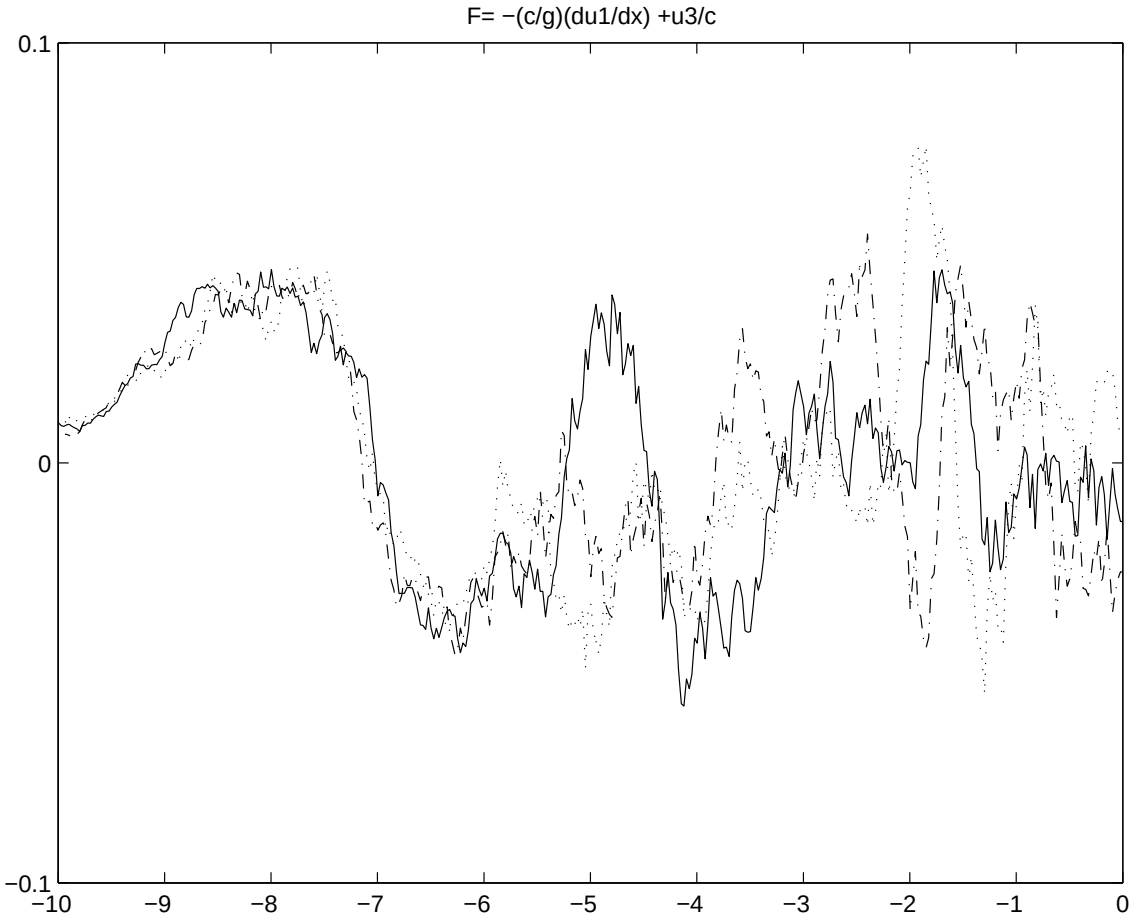

Figur 3: Three realizations of the F-faktor estimated on a grid resolution of $\triangle x_1 \approx 180$m. The moderate grid resolution turns out to underestimate $\sqrt{K}$ by at least a factor of 1.5, so that the F-factor is also underestimated by this factor (Equation 16). Commonly applied alert- and warning- levels are: $F < -0.05$ and $F < -0.1$ respectively.